

# RSC Advances



This is an *Accepted Manuscript*, which has been through the Royal Society of Chemistry peer review process and has been accepted for publication.

*Accepted Manuscripts* are published online shortly after acceptance, before technical editing, formatting and proof reading. Using this free service, authors can make their results available to the community, in citable form, before we publish the edited article. This *Accepted Manuscript* will be replaced by the edited, formatted and paginated article as soon as this is available.

You can find more information about *Accepted Manuscripts* in the [Information for Authors](#).

Please note that technical editing may introduce minor changes to the text and/or graphics, which may alter content. The journal's standard [Terms & Conditions](#) and the [Ethical guidelines](#) still apply. In no event shall the Royal Society of Chemistry be held responsible for any errors or omissions in this *Accepted Manuscript* or any consequences arising from the use of any information it contains.

## Theoretical Studies on the Photoisomerization Mechanism of Osmium(II) Sulfoxide Complexes

Huifang Li<sup>\*a</sup>, Lisheng Zhang<sup>a</sup>, Yanfei Wang<sup>a</sup>, Xiaolin Fan<sup>\*ab</sup>

<sup>a</sup>Key Laboratory of Organo-Pharmaceutical Chemistry, Gannan Normal University, Ganzhou 341000, R. R. China.

<sup>b</sup>Material and Chemical Engineering Department, Pingxiang University, Pingxiang 337055, R. R. China.

**ABSTRACT** Photochromic compounds, employing photonic energy for excited-state bond rupture and bond construction processes, are excellent candidates for the application as optical molecular information storage devices. In this work, a dispersion corrected density functional theory (DFT-D) study was carried out on the photoisomerization mechanism of osmium sulfoxide complex,  $[\text{Os}(\text{bpy})_2(\text{DMSO})_2]^{2+}$  (bpy = 2,2'-bipyridine; DMSO = dimethyl sulfoxide), which features a pronounced photochromic character based on an ultrafast photo-triggered linkage isomerization located at the SO-ligand. Calculated results demonstrate that the Os-S→Os-O isomerization proceeds adiabatically on the potential energy surface (PES) of the lowest metal-to-ligand charge transfer excited states  ${}^3\text{MLCT}_\text{S}\rightarrow{}^3\text{MLCT}_\text{O}$ , and the metal centered ligand field ( ${}^3\text{LF}_\text{S}$ ) excited state is not involved. However, attributed to the weakened Os-DMSO bond-strength upon Os-S to Os-O isomerization, population of the  ${}^3\text{LF}_\text{O}$  excited state is thermally accessible. Therefore, photodissociation of DMSO from Os center occurs via homolytic cleavage of Os-O bond after an avoided curve crossing between the lowest  ${}^3\text{MLCT}_\text{O}$  state and the  ${}^3\text{LF}_\text{O}$  repulsive state along the stretching coordinate of the Os-O bond.

**KEYWORDS:** Osmium Sulfoxide Complexes:  $[\text{Os}(\text{bpy})_2(\text{DMSO})_2]^{2+}$ ; Intrinsic Reaction Paths: Photoisomerization Mechanism: Dispersion Corrected Density Functional Theory

\* To whom correspondence should be addressed. E-mail: [huifang0801@gmail.com](mailto:huifang0801@gmail.com) (H. F. Li), [fanxl@gnnu.edu.cn](mailto:fanxl@gnnu.edu.cn) (X. L. Fan).

## 1. Introduction

Due to their excited-state bond rupture and bond construction characters, photochromic complexes based on  $d^6$  transition metal complexes are promising and versatile candidates for the applications in light energy storage and light-activated switches.<sup>1-6</sup> Among them, polypyridine ruthenium(II)<sup>7-10</sup> and osmium(II)<sup>11,12</sup> sulfoxide complexes, in which the intramolecular isomerization of the coordinated sulfoxide group from  $M^{n+}$ -S to  $M^{n+}$ -O linkage mode can be triggered by external light signal, are highly appealing and have attracted a great deal of attention.

Intramolecular isomerization of the sulfoxide group in polypyridine ruthenium(II) complexes was firstly observed for  $[\text{Ru}(\text{bpy})_2(\text{DMSO})_2]^{2+}$  (bpy = 2,2'-bipyridine; DMSO = dimethyl sulfoxide) by the group of F. R. Keene.<sup>13</sup> In their studies, a color change from yellow to red was observed due to the photo-induced one DMSO ligand isomerization upon exposure to sunlight or UV irradiation. Soon afterwards, photochromic character of osmium sulfoxide complexes was reported by the group of J. J. Rack.<sup>14</sup> In their studies, photo-induced one DMSO ligand isomerization was observed in  $[\text{Os}(\text{bpy})_2(\text{DMSO})_2]^{2+}$ , as displayed in Figure 1. Correspondingly, their absorption maximum was shifted from 355 nm to a new peak 403 nm by such molecular rearrangement. In the last few years, many investigations have been devoted to the synthesis and characterization studies for such polypyridine ruthenium or osmium complexes with photoisomerizable sulfoxide group.<sup>15-22</sup> Except for experimental achievements, theoretical studies have also been carried out for exploring the electronic and photophysical properties of such transition-metal based chromophores.<sup>23-27</sup> It is found that the HOMO-LUMO energy gap is decreased by  $M^{n+}$ -S $\rightarrow$  $M^{n+}$ -O linkage isomerization due to the decreased electron transfer amount from surrounding ligands to central  $M^{n+}$ , which makes the absorption of such photochromic ruthenium(II) or osmium(II) sulfoxide complexes red shifted.<sup>26</sup>

It has been realized that quite different excited-state characters can be formed after one-electron excitation from the ground state ( $^1\text{GS}$ ) attributed to the different orbital parentage.<sup>28</sup> The potential energies of the ground state and two triplet states are displayed in the model diagram, Figure 2. The two triplet states are the

metal-to-ligand charge transfer ( ${}^3\text{MLCT}$ ) and the metal centered excited ligand field ( ${}^3\text{LF}$ ) excited state. Among them,  ${}^3\text{MLCT}$  indicates the lowest excited triplet state of transition-metal complexes formed by promotion of an electron from a  $\pi_{\text{M}}$  metal orbital to the  $\pi_{\text{L}}^*$  ligand orbitals, which exhibits long lifetime and intense luminescence emission.  ${}^3\text{LF}$  indicates a higher triplet energy involving the bonding and antibonding orbitals of a  $\text{M}^{n+}\text{-L}$  bond between surrounding ligand and  $\text{M}^{n+}$  center, which often leads to fast radiationless decay to the ground state/or ligand dissociation reactions. According to previous report,  ${}^3\text{MLCT}$  excited state will be raised inevitably to a region very close to or even higher than the upper lying  ${}^3\text{LF}$  excited state by the dissociation along the  $\text{M}^{n+}\text{-L}$  bond.<sup>28</sup> Then, these two states mix and intersect, which is called avoided crossing. If the energy barrier ( $E_{\text{a}}$ ) from left to right can be overcome,  ${}^3\text{LF}$  becomes the lowest triplet state in the stretched  $\text{M}^{n+}\text{-L}$  bond region instead of  ${}^3\text{MLCT}$  in the equilibrium geometry region on the left of avoided crossing. As a result, the transition-metal complexes will undergo fast homolytic dissociation following the repulsive  ${}^3\text{LF}$  curve. It has been demonstrated that  ${}^3\text{LF}$  excited states play a central role in the photoisomerization mechanism of photochromic polypyridine ruthenium sulfoxide complexes.<sup>27</sup> Thereby, nonadiabatic pathways for such photoisomerization process in photochromic  $[\text{Ru}(\text{bpy})_2(\text{OSO})]^+$  can be explained due to their fast radiationless decay to the ground state from the  ${}^3\text{LF}$  states.<sup>8</sup>

However, it is still unclear that whether the  ${}^3\text{LF}$  excited state is involved in the photoisomerization mechanism of osmium sulfoxide complexes or not. For better understanding the extra-light triggered intramolecular isomerization mechanism of osmium sulfoxide complexes, intrinsic reaction pathways (IRPs) for the  $\text{Os-S}_1 \rightarrow \text{Os-O}_1$  and  $\text{Os-O}_1 \rightarrow \text{Os-S}_1$  processes in ground and excited states of  $[\text{Os}(\text{bpy})_2(\text{DMSO})_2]^{2+}$  complex were examined theoretically.

## 2. Computational Details

Considering  $\text{Os-S}$  and  $\text{Os-O}$  bonds are weak interactions and the bond lengths are overestimated by current density functional theory, the empirical dispersion correction<sup>29</sup> was added to the density functional theory (DFT) with Becke's and

Johnson's rational damping function<sup>30</sup> in optimization calculations, and dubbed this variant DFT-D3(BJ). Based on the results from a number of benchmark calculations, collected in Table S1, the appropriate PBE0<sup>31</sup>-D3(BJ) exchange correlation functional was employed for the fully gradient optimization of the osmium complexes. Two basis set (BS1 and BS2) was considered. BS1 is made of SDD<sup>32</sup> for osmium, a correlation-consistent polarized double- $\zeta$  basis set (cc-pVDZ)<sup>33</sup> for H atoms, and a correlation-consistent polarized triple- $\zeta$  basis set (cc-pVTZ)<sup>33</sup> for C, N, O and S atoms. BS2 is made of pseudopotential-based augmented correlation-consistent basis set (aug-cc-pVDZ-pp)<sup>34</sup> for osmium and aug-cc-pVDZ for non-metal atoms. In addition, conductor-like polarizable continuum model (CPCM)<sup>35</sup> using solvent acetonitrile ( $\epsilon=35.688$ ) was also considered for optimization calculations of the involved geometries. Harmonic vibrational frequencies were calculated analytically at the same level to ascertain the nature of the optimized structures. The QST3 algorithm was employed for the location of the transition structures (TS) which were confirmed by having only one imaginary frequency with the corresponding eigenvector pointing toward the reactants and products. In addition, intrinsic reaction coordinate (IRC)<sup>36,37</sup> calculations were also performed to make sure that the optimized transition states were connected with two relevant minima.

To shed light on the nature of the excited states of the S- and O-linked osmium complexes, vertical transition energies were calculated on the basis of the optimized S0 and T1 structures via time-dependent DFT (TD-DFT)<sup>38</sup> at the same level (BS1) which promises a way forward to study excited states of large metallic complexes. Natural transition orbital (NTO)<sup>39</sup> analyses were performed to examine the nature of the excited states.

Charge distribution was evaluated with the natural population analysis (NPA)<sup>40</sup> for the aim to examine the degree of charge transfer between surrounding ligands and central osmium.

All calculations were performed by using the Gaussian 09 package.<sup>41</sup>

### 3. Results and Discussion

Photo-induced one DMSO ligand isomerization upon exposure to sunlight or UV irradiation has been observed experimentally in polypyridine osmium(II) complex,  $[\text{Os}(\text{bpy})_2(\text{DMSO})_2]^{2+}$ .<sup>14</sup> Chemical structures of these two different isomers with  $S_1$ - and  $O_1$ -linkage mode are displayed in Figure 1. Optimized geometrical parameters are collected in Table 1, available experimental results<sup>14</sup> are also included for comparison. A good agreement between them can be obtained. NPA charge distribution results for these isomers in the ground and excited states are listed in Table 2. Calculated reaction energies as well as energy barriers for the intramolecular bond rupture and bond construction processes in  $[\text{Os}(\text{bpy})_2(\text{DMSO})_2]^{2+}$  are given in Table 3. It is found that the influences of the electron density redistribution induced by one-electron excitation on the intrinsic reaction paths (IRPs) of intramolecular isomerization of  $[\text{Os}(\text{bpy})_2(\text{DMSO})_2]^{2+}$  are significantly.

### 3.1. Os–Sulfoxide Bond-Strength Changes upon One-Electron Excitation

As listed in Table 1, optimized Os- $S_1$  bond in the ground state ( $^1\text{GS}_S$ ) of  $S_1$ - $[\text{Os}(\text{bpy})_2(\text{DMSO})_2]^{2+}$  is 2.286 Å, which is shorter than that in the metal-to-ligand charge transfer excited state ( $^3\text{MLCT}_S$ ) by about 0.095 Å. On the contrary, the Os- $O_1$  bond in the  $^1\text{GS}_O$  state is longer than that in the  $^3\text{MLCT}_O$  state for about 0.089 Å. It means the Os- $S_1$  bond is weakened, while Os- $O_1$  bond is strengthened upon one-electron excitation.

Frontier molecular orbitals (MOs) play an important role in photoresponsive materials because location of the highest occupied molecular orbital (HOMO) and the lowest unoccupied molecular orbital (LUMO) is quite reasonable for the description of the first excited singlet transition. As shown in Figure 3, for these  $[\text{Os}(\text{bpy})_2(\text{DMSO})_2]^{2+}$  isomers, the HOMO is mainly distributed on central osmium, while the LUMO is mainly distributed on the bpy ligands. Thereby, the  $^3\text{MLCT}_S$  and  $^3\text{MLCT}_O$  excited states were formed with one-electron promotion from a  $\pi_{\text{Os}}$  metal orbital to the  $\pi_{\text{bpy}}^*$  bpy ligand orbitals. Electron configuration and singly occupied molecular orbitals of the excited states are shown in Figure 4. NPA charge calculation results demonstrate that the charge distributed on central osmium is decreased by

0.394 and 0.413 e, respectively, upon one-electron excitation from  $S_1$ - and  $O_1$ -linked isomers.

As known, S-bonding is favored in the case of ‘soft’ metal atoms where the sulfoxides act as moderate  $\pi$ -acceptor ligands,<sup>42</sup> so that the metal to sulfur bond is strengthened when electron distribution on central metal is increased. Thereby, weakened Os– $S_1$  bond upon one-electron excitation from a  $\pi_{Os}$  orbital to the  $\pi_{bpy}^*$  orbitals can be explained. Differently, it has been proved that O-bonding is favored in the case of ‘hard’ metal atoms where the sulfoxides act as moderate  $\sigma$ -donor ligands, so that the metal-oxygen bond is strengthened when electron distribution on central metal is decreased. Thereby, the Os– $O_1$  bond is strengthened by one-electron excitation from a  $\pi_{Os}$  orbital to the  $\pi_{bpy}^*$  orbitals.

The variation trends of the S–O bond distances are also rationalized considering the metal–sulfoxide bonding changes upon one-electron excitation. As listed in Table 2, the weakened Os– $S_1$  bond-strength reduces the positive charge of sulfur atom from 1.594 to 1.568 e, and thus the electronegativity of  $S_1$  atom is decreased. Therefore, there is additional electron transfer from  $O_1$  to  $S_1$  (the charge on  $O_1$  is decreased from -0.952 to -0.931 e) for compensation, which leads to the increased double bond character of the  $S_1$ – $O_1$ . As a result, the  $S_1$ – $O_1$  bond in the ground state of  $S_1$ -[Os(bpy)<sub>2</sub>(DMSO)<sub>2</sub>]<sup>2+</sup> (<sup>1</sup>GS<sub>S</sub>) is decreased from 1.494 to 1.481 Å upon one-electron excitation. For the  $O_1$ -linked isomer, the charge on  $O_1$  atom is changed from -0.856 to -0.818 e by one-electron excitation, which makes the electronegativity of  $O_1$  atom increased. Due to the equalization of atom electronegativities,<sup>43</sup> this is compensated by electron transfer from the sulfur atom and the methyl groups which makes the positive charge on the  $S_1$  atom decreased from 1.228 to 1.218 e. Furthermore, attributed to the increased  $O_1$  electronegativity, the  $\pi$ -electron transfer from  $O_1$  to  $S_1$  is decreased. As a result, the S–O bond-strength is weakened and its bond-length is increased from 1.551 to 1.574 Å.

### 3.2. Intrinsic Reaction Paths

As shown in Figure 5,  $S_1$ -[Os(bpy)<sub>2</sub>(DMSO)<sub>2</sub>]<sup>2+</sup> is stable than its  $O_1$ -linked isomer,  $O_1$ -[Os(bpy)<sub>2</sub>(DMSO)<sub>2</sub>]<sup>2+</sup>, for about 0.20 eV because Os–S linkage mode of DMSO is preferred in the ground state of Os(II) complex. Energy barrier for the isomerization from S- to O-linkage is about 1.08 eV. Computational results demonstrated that the energy barrier between  $S_1$ - and  $O_1$ -linked isomers in the lowest excited states is lower than that in the ground states by about 0.92 eV. It means such intramolecular isomerization process should be much easier to proceed in the lowest excited state. Thereby, stimulated by external light, one DMSO ligand isomerization from Os–S<sub>1</sub> to Os–O<sub>1</sub> linkage mode in [Os(bpy)<sub>2</sub>(DMSO)<sub>2</sub>]<sup>2+</sup> was observed in experimental studies. As mentioned above, the Os–S<sub>1</sub> bond is weakened and the Os–O<sub>1</sub> bond is strengthened by electron density redistribution upon one-electron excitation, which makes the energy of  $S_1$ -[Os(bpy)<sub>2</sub>(DMSO)<sub>2</sub>]<sup>2+</sup> higher than  $O_1$ -[Os(bpy)<sub>2</sub>(DMSO)<sub>2</sub>]<sup>2+</sup> by about 0.36 eV in the lowest <sup>3</sup>MLCT excited states. As a result, the Os–S<sub>1</sub> to Os–O<sub>1</sub> isomerization process is changed from endothermic to exothermic reaction upon one-electron excitation. However, calculated results show that the  $S_1$ -[Os(bpy)<sub>2</sub>(DMSO)<sub>2</sub>]<sup>2+</sup> in the lowest <sup>3</sup>MLCT excited state is stable than that in the <sup>3</sup>LF<sub>S</sub> state for about 0.16 eV. This means <sup>3</sup>MLCT<sub>S</sub>→<sup>3</sup>MLCT<sub>O</sub> isomerization is more thermodynamically favored in the excited state compared with the <sup>3</sup>MLCT<sub>S</sub>→<sup>3</sup>LF<sub>S</sub> pathways.

It is obvious that the photoisomerization mechanism of ruthenium sulfoxide complex, [Ru(bpy)<sub>2</sub>(OSO)]<sup>+</sup>, is different with that of [Os(bpy)<sub>2</sub>(DMSO)<sub>2</sub>]<sup>2+</sup>. As reported by A. J. Göttle and his coworkers, <sup>3</sup>LF state plays a central role in the Ru–S→Ru–O nonadiabatic photoisomerization mechanism of [Ru(bpy)<sub>2</sub>(OSO)]<sup>+</sup> complexes.<sup>27</sup> Thereby, no O-bonded excited state, <sup>3</sup>MLCT<sub>O</sub>, of [Ru(bpy)<sub>2</sub>(OSO)]<sup>+</sup> complex can be observed experimentally.<sup>8</sup> It is proposed that the <sup>3</sup>LF<sub>S</sub> excited state is more stable than the <sup>3</sup>MLCT<sub>O</sub> state. Thereby, the <sup>3</sup>LF<sub>S</sub> excited state in [Ru(bpy)<sub>2</sub>(OSO)]<sup>+</sup> should be thermally accessible from the initial radiative <sup>3</sup>MLCT<sub>S</sub> electron state and no <sup>3</sup>MLCT<sub>O</sub> excited state of [Ru(bpy)<sub>2</sub>(OSO)]<sup>+</sup> complex was observed.

Differently, along with the Os-O bond rupture in the lowest  ${}^3\text{MLCT}_\text{O}$  excited state of  $O_1\text{-}[\text{Os}(\text{bpy})_2(\text{DMSO})_2]^{2+}$ , instead of Os-S bond construction, a new  $O_1$ -linked osmium complex in the  ${}^3\text{LF}_\text{O}$  state is formed. Optimized geometrical parameters of the  $O_1\text{-}[\text{Os}(\text{bpy})_2(\text{DMSO})_2]^{2+}$  in the  ${}^3\text{LF}_\text{O}$  state are listed in Table 1. It means, for the excited-state Os-O bond breaking process, nonradiative  ${}^3\text{LF}_\text{O}$  excited state should be accessible from the initial radiative  ${}^3\text{MLCT}_\text{O}$  electron state. As shown in Figure 6, it is because the energy barrier for the  ${}^3\text{MLCT}_\text{O}\rightarrow{}^3\text{LF}_\text{O}$  process (0.41 eV) is smaller than that for the  ${}^3\text{MLCT}_\text{O}\rightarrow{}^3\text{MLCT}_\text{S}$  pathway (0.56 eV). Considering promotion to the  ${}^3\text{LF}$  state often leads to fast radiationless decay to the ground state or ligand dissociation reactions,<sup>44</sup> it can be predicted that photodissociation of DMSO from Os center may occur via homolytic cleavage of Os-O bond after an avoided curve crossing between the lowest  ${}^3\text{MLCT}_\text{O}$  state and a  ${}^3\text{LF}$  repulsive state along the stretching mode of the Os-O bond.

This can be confirmed with TD-DFT calculation results. As shown in the Figure 7 and Table S2, NTO results demonstrated that the first transition ( $S_1$ ) of  $S\text{-}[\text{Os}(\text{bpy})_2(\text{DMSO})_2]^{2+}$  is from the ground state ( ${}^1\text{GS}_\text{S}$ ) to  ${}^1\text{MLCT}$  (formed with  $\pi_\text{L}^*$  ligand orbitals and  $d_{xy}$ ,  $d_{yz}$  or  $d_{xz}$  metal orbitals) and the third transition ( $S_3$ ) is from  ${}^1\text{GS}_\text{S}$  to  ${}^1\text{LF}_\text{S}$  (formed with  $\pi_\text{L}^*$  ligand orbitals and  $d_{x^2-y^2}$  or  $d_{z^2}$  metal orbitals). For  $O\text{-}[\text{Os}(\text{bpy})_2(\text{DMSO})_2]^{2+}$ , the  $S_1$  is from  ${}^1\text{GS}_\text{O}$  to  ${}^1\text{MLCT}_\text{O}$  and the  $S_2$  is from  ${}^1\text{GS}_\text{O}$  to  ${}^1\text{LF}_\text{O}$ . The energy gap between  ${}^1\text{MLCT}_\text{S}$  and  ${}^1\text{LF}_\text{S}$  is lower than that between  ${}^1\text{MLCT}_\text{O}$  and  ${}^1\text{LF}_\text{O}$  (0.28 eV). This is in good agreement with DFT calculation results. More importantly, from TD-DFT results, it is observed that the  ${}^1\text{MLCT}_\text{O}$  excited state is more stable than the  ${}^1\text{MLCT}_\text{S}$  excited state. Moreover, the energy of the  ${}^1\text{LF}_\text{O}$  excited state is lower than that of the  ${}^1\text{MLCT}_\text{S}$  excited state. This can be used for better understanding that why the  $\text{Os-S}_1\rightarrow\text{Os-O}_1$  isomerization proceeds adiabatically on the PES of  $\text{MLCT}_\text{S}\rightarrow\text{MLCT}_\text{O}$  and the  $\text{LF}_\text{S}$  excited state is not involved. Differently, for the excited-state Os-O bond breaking process, nonradiative  $\text{LF}_\text{O}$  excited state should be accessible from the initial radiative  $\text{MLCT}_\text{O}$  excited state.

#### 4. Conclusion

A DFT-D study was carried out on the photo-triggered intramolecular linkage isomerization of osmium sulfoxide complex,  $[\text{Os}(\text{bpy})_2(\text{DMSO})_2]^{2+}$ , for better understanding the photoisomerization mechanism of osmium complexes as well as the role of the  $^3\text{LF}$  excited state in the bond rupture ( $\text{M}^{n+}\text{-X}$ ) and bond construction ( $\text{M}^{n+}\text{-Y}$ ) processes.

The metal-to-ligand charge transfer excited states ( $^3\text{MLCT}_\text{S}$  and  $^3\text{MLCT}_\text{O}$ ) were formed by one-electron promotion from a  $\pi_{\text{Os}}$  metal orbital to the  $\pi_{\text{bpy}}^*$  bpy ligand orbitals which makes the electron distribution on central osmium decreased. As a consequence, the Os-S<sub>1</sub> bond is weakened because S-bonding is favored in the case of 'soft' metal atoms, while the Os-O<sub>1</sub> bond is strengthened because O-bonding is favored in the case of 'hard' metal atoms. As a result, the Os-S<sub>1</sub> to Os-O<sub>1</sub> isomerization process is changed from endothermic to exothermic reaction upon one-electron excitation. It means such intramolecular isomerization process should be much easier to proceed in the lowest excited state.

Moreover, it is found that the Os-S<sub>1</sub>→Os-O<sub>1</sub> isomerization proceeds adiabatically on the PES of  $^3\text{MLCT}_\text{S}$ → $^3\text{MLCT}_\text{O}$ , and the  $^3\text{LF}_\text{S}$  state is not involved. Differently, along with the Os-O bond rupture in the lowest  $^3\text{MLCT}_\text{O}$  excited state of  $O_1$ - $[\text{Os}(\text{bpy})_2(\text{DMSO})_2]^{2+}$ , no Os-S bond construction is observed and a new  $O_1$ -linked osmium complex in the  $^3\text{LF}_\text{O}$  state is formed. It means, for the excited-state Os-O bond breaking process, nonradiative  $^3\text{LF}_\text{O}$  excited state should be accessible from the initial radiative  $^3\text{MLCT}_\text{O}$  electron state. As a result, photodecomposition of the DMSO ligand from the  $^3\text{LF}_\text{O}$  excited state complex may occur along with the Os-O bond stretching mode because promotion to the  $^3\text{LF}$  state often leads to fast radiationless decay to the ground state or ligand dissociation reactions.

**Electronic supplementary information (ESI) available:** Benchmark calculations. TD-DFT results. Optimized Cartesian coordinates, electronic structures, energies of all stationary points and partial optimization results.

**Acknowledgements**

This work is supported by the National Natural Science Foundation of China (21403037, 51478123, 21463003), the Natural Science Foundation of Jiangxi Province (20142BAB213014), Jiangxi Provincial “Ganpo Talents 555 Projects” and the Scientific Research Foundation for the Returned Overseas Chinese Scholars, State Education Ministry, PR China.

## References

- 1 N. V. Mockus, D. Rabinovich, J. L. Petersen, J. J. Rack, *Angew. Chem. Int. Ed.* **2008**, *47*, 1458–1461.
- 2 M. N. Roberts, C-J. Carling, J. K. Nagle, N. R. Branda, M. O. Wolf, *J. Am. Chem. Soc.*, **2009**, *131*, 16644–16645.
- 3 T. Ishizuka, T. Sawaki, S. Miyazaki, M. Kawano, Y. Shiota, K. Yoshizawa, S. Fukuzumi, T. Kojima, *Chem. Eur. J.* **2011**, *17*, 6652–6662.
- 4 S. Bonnet, J-P. Collin, *Chem. Soc. Rev.*, **2008**, *37*, 1207–1217.
- 5 V. Marin, E. Holder, R. Hoogenboom, U. S. Schubert. *Chem. Soc. Rev.*, **2007**, *36*, 618–635.
- 6 K. Garg, A. W. King, J. J. Rack, *J. Am. Chem. Soc.*, **2014**, *136*, 1856–1863.
- 7 B. A. McClure, N. V. Mockus, D. P. Butcher, Jr., D. A. Lutterman, C. Turro, J. L. Petersen, J. J. Rack, *Inorg. Chem.* **2009**, *48*, 8084–8091.
- 8 B. A. McClure, E. R. Abrams, J. J. Rack, *J. Am. Chem. Soc.* **2010**, *132*, 5428–5436.
- 9 A. A. Rachford, J. J. Rack, *J. Am. Chem. Soc.* **2006**, *128*, 14318–14324.
- 10 B. A. McClure, J. J. Rack, *Inorg. Chem.* **2011**, *50*, 7586–7590.
- 11 J. J. Rack, *Coord. Chem. Rev.* **2009**, *253*, 78–85.
- 12 K. Garg, S. I. M. Paris, J. J. Rack, *Eur. J. Inorg. Chem.* **2013**, 1142–1148.
- 13 M. K. Smith, J. A. Gibson, C. G. Young, J. A. Broomhead, P. C. Junk, F. R. Keene, *Eur. J. Inorg. Chem.* **2000**, 1365–1370.
- 14 a) N. V. Mockus, J. L. Petersen, J. J. Rack, *Inorg. Chem.* **2006**, *45*, 8–10; b) B. A. McClure, J. J. Rack, *Eur. J. Inorg. Chem.* **2010**, 3895–3904.
- 15 N. V. Mockus, S. Marquard, J. J. Rack, *J. Photoch. Photobio. A*, **2008**, *200*, 39–43.
- 16 A. W. King, Y. Jin, J. T. Engle, C. J. Ziegler, J. J. Rack, *Inorg. Chem.* **2013**, *52*, 2086–2093.
- 17 A. A. Rachford, J. L. Petersen, J. J. Rack, *Dalton Trans.*, **2007**, 3245–3251.
- 18 A. E. Phillips, J. M. Cole, T. d’Almeida, K. S. Low, *Inorg. Chem.* **2012**, *51*, 1204–1206.
- 19 B. A. McClure, J. J. Rack, *Angew. Chem. Int. Ed.* **2009**, *48*, 8556–8558.
- 20 B. L. Portera, B. A. McClure, E. R. Abrams, J. T. Engle, C. J. Ziegler, J. J. Rack, *J. Photoch. Photobio. A*, **2011**, *217*, 341–346.
- 21 A. A. Rachford, J. L. Petersen, J. J. Rack, *Inorg. Chem.* **2006**, *45*, 5953–5960.
- 22 D. P. Butcher, A. A. Rachford, J. L. Petersen, J. J. Rack, *Inorg. Chem.* **2006**, *45*, 9178–9180.

- 23 I. Ciofini, C. A. Daul, C. Adamo, *J. Phys. Chem. A* **2003**, *107*, 11182–11190.
- 24 D. A. Lutterman, A. A. Rachford, J. J. Rack, C. Turro, *J. Phys. Chem. A* **2009**, *113*, 11002–11006.
- 25 a) H. F. Li, L. S. Zhang, H. Lin, X. L. Fan, *RSC Adv.*, **2014**, *4*, 45635–45640; b) H. F. Li, L. S. Zhang, H. Lin, X. L. Fan, *Chem. Phys. Lett.*, **2014**, *604*, 10–14.
- 26 H. F. Li, L. S. Zhang, X. L. Fan, Y. Zhao. *J. Phys. Chem. A* **2015**, *119*, 4244–4251.
- 27 A. J. Göttle, I. M. Dixon, F. Alary, J-L. Heully, M. Boggio-Pasqua, *J. Am. Chem. Soc.* **2011**, *133*, 9172–9174.
- 28 a) S. Bonnet, J. P. Collin, *Chem. Soc. Rev.*, 2008, **37**, 1207–1217; b) Q. Sun, S. Mosquera-Vazquez, L. M. L. Daku, L. Guénée, H. A. Goodwin, E. Vauthey, A. Hauser, *J. Am. Chem. Soc.* 2013, **135**, 13660–13663; c) J. T. Hewitt, J. J. Concepcion, N. H. Damrauer, *J. Am. Chem. Soc.* 2013, **135**, 12500–12503
- 29 a) S. Grimme, J. Antony, S. Ehrlich, H. Krieg, *J. Chem. Phys.* **2010**, *132*, 154104; b) L. Goerigk, S. Grimme, *Phys. Chem. Chem. Phys.* **2011**, *13*, 6670–6688.
- 30 a) A. D. Becke, and E. R. Johnson, *J. Chem. Phys.* **2005**, *123*, 154101; b) E. R. Johnson, and A. D. Becke, *J. Chem. Phys.* **2005**, *123*, 024101; c) E. R. Johnson, and A. D. Becke, *J. Chem. Phys.* **2006**, *124*, 174104.
- 31 C. Adamo, V. Barone, *J. Chem. Phys.* **1999**, *110*, 6158–6170.
- 32 D. Andrae, U. Häussermann, M. Dolg, H. Stoll, H. Preuss, *Theor. Chim. Acta.* **1990**, *77*, 123–141.
- 33 T. H. Dunning, *J. Chem. Phys.* **1989**, *90*, 1007–1023.
- 34 K. A. Peterson, C. Puzzarini, *C. Theor. Chem. Acc.* **2005**, *114*, 283–296.
- 35 V. Barone, M. Cossi, *J. Phys. Chem. A* **1998**, *102*, 1995–2001.
- 36 K. Fukui, *Acc. Chem. Res.* **1981**, *14*, 363–368.
- 37 H. P. Hratchian, H. B. Schlegel, *J. Chem. Phys.* **2004**, *120*, 9918–9924.
- 38 S. Fantacci, F.D. Angelis, A. Selloni, *J. Am. Chem. Soc.* **2003**, *125*, 4381–4387.
- 39 R.L. Martin, V. Affiliations, *J. Chem. Phys.* **2003**, *118*, 4775–4777.
- 40 A. E. Reed, L. A. Curtiss, F. Weinhold, *Chem. Rev.* **1988**, *88*, 899–926.
- 41 M. J. Frisch, G. W. Trucks, H. B. Schlegel, G. E. Scuseria, M. A. Robb, J. R. Cheeseman, G. Scalmani, V. Barone, B. Mennucci, G. A. Petersson, H. Nakatsuji, M. Caricato, X. Li, H. P. Hratchian, A. F. Izmaylov, J. Bloino, G. Zheng, J. L. Sonnenberg, M. Hada, M. Ehara, K. Toyota, R. Fukuda, J. Hasegawa, M. Ishida, T. Nakajima, Y. Honda, O. Kitao, H. Nakai, T. Vreven, J. A. Montgomery, Jr., J. E. Peralta, F. Ogliaro, M. Bearpark, J. J. Heyd, E. Brothers, K. N. Kudin, V. N. Staroverov, T. Keith, R. Kobayashi, J. Normand, K. Raghavachari, A. Rendell, J. C. Burant, S. S. Iyengar, J. Tomasi, M. Cossi, N. Rega, J. M. Millam, M. Klene, J. E. Knox, J. B. Cross, V. Bakken, C. Adamo, J. Jaramillo, R. Gomperts, R. E. Stratmann, O. Yazyev, A. J. Austin, R. Cammi, C. Pomelli, J. W. Ochterski, R. L. Martin, K. Morokuma, V. G. Zakrzewski, G. A. Voth, P. Salvador, J. J. Dannenberg, S. Dapprich, A. D. Daniels, O. Farkas, J. B. Foresman, J. V. Ortiz, J. Cioslowski, and D. J. Fox, Gaussian 09, Revision D.01, Gaussian, Inc.; Wallingford CT, **2013**.

- 42 M. Calligaris, *Coord. Chem. Rev.*, **2004**, *248*, 351–375.
- 43 W.J. Mortier, *Struct. Bonding* 1987, **66**, 125. b) R.T. Sanderson, *J. Chem. Ed.* **1954**, *31*, 2.
- 44 a) P. S. Wagenknecht, P. C. Ford, *Coord. Chem. Rev.* **2011**, *255*, 591–616. b) Q. Sun, S. Mosquera-Vazquez, L. M. L. Daku, L. Guénée, H. A. Goodwin, E. Vauthey, A. Hauser, *J. Am. Chem. Soc.* **2013**, *135*, 13660–13663. c) J. T. Hewitt, J. J. Concepcion, N. H. Damrauer, *J. Am. Chem. Soc.* **2013**, *135*, 12500–12503.

**Table 1.** Calculated bond lengths (angstroms) and bond angles (degrees) for Os(II) complexes, as determined at the PBE0-D3(BJ)/BS2 level of theory. Optimizations are conducted in acetonitrile by using the CPCM model.

Bond	<i>S-bonded</i>				<i>O-bonded</i>		
	<sup>1</sup> GS <sub>S</sub>	Exptl. <sup>a</sup>	<sup>3</sup> MLCT <sub>S</sub>	<sup>3</sup> LF <sub>S</sub>	<sup>1</sup> GS <sub>O</sub>	<sup>3</sup> MLCT <sub>O</sub>	<sup>3</sup> LF <sub>O</sub>
Os-S <sub>1</sub>	2.286	2.276	2.381	2.832	—	—	—
Os-O <sub>1</sub>	—	—	—	—	2.147	2.058	2.830
S <sub>1</sub> -O <sub>1</sub>	1.494	1.471	1.481	1.512	1.551	1.574	1.521
Os-S <sub>2</sub>	2.286	2.268	2.342	2.304	2.271	2.345	2.292
S <sub>2</sub> -O <sub>2</sub>	1.494	1.477	1.483	1.494	1.491	1.482	1.492
Os-N <sub>b1</sub>	2.009	2.100	2.118	2.131	2.067	2.083	2.145
Os-N <sub>b1</sub> '	2.101	2.091	2.101	2.246	2.038	2.052	2.268
Os-N <sub>b2</sub>	2.101	2.097	2.076	2.091	2.088	2.078	2.089
Os-N <sub>b2</sub> '	2.009	2.094	2.024	2.071	2.094	2.086	2.059
$\alpha(\text{O}_1\text{-S}_1\text{-Os})/\alpha(\text{S}_1\text{-O}_1\text{-Os})$	116.0	115.8	113.5	77.0	120.6	123.6	116.8
$\alpha(\text{S}_1\text{-Os-Nb}_1)/(\text{O}_1\text{-Os-Nb}_1)$	98.0	97.8	99.6	95.6	91.4	91.1	83.8
$\alpha(\text{O}_2\text{-S}_2\text{-Os})$	116.3	116.0	115.2	118.1	117.9	118.4	117.9

<sup>a</sup> Ref. 14.

**Table 2.** Natural population charges distributed on the Os complexes (Q)<sup>a</sup>.

	<i>S-bonded</i>			<i>O-bonded</i>		
	<sup>1</sup> GS <sub>S</sub>	<sup>3</sup> MLCT <sub>S</sub>	<sup>3</sup> LF <sub>S</sub>	<sup>1</sup> GS <sub>O</sub>	<sup>3</sup> MLCT <sub>O</sub>	<sup>3</sup> LF <sub>O</sub>
S <sub>1</sub>	1.594	1.568	1.204	1.228	1.218	1.218
O <sub>1</sub>	-0.952	-0.931	-1.007	-0.856	-0.818	-0.991
Os	-0.443	-0.049	0.353	-0.062	0.351	0.355
DMSO1	0.569	0.634	0.064	0.330	0.407	0.121
DMSO2	0.569	0.577	0.479	0.519	0.592	0.467
BPY1	0.652	0.696	0.523	0.619	0.018	0.497
BPY2	0.652	0.142	0.581	0.594	0.631	0.560

<sup>a</sup> Q(ligand) indicates the charge on all the atoms in ligand.

**Table 3.** Energy parameters associated with the intramolecular isomerization in  $[\text{Os}(\text{bpy})_2(\text{DMSO})_2]^{2+}$  obtained at the PBE0-D3(BJ)/BS1 and PBE0-D3(BJ)/BS2 level of theory. (Energies are in eV.)

	BS1		BS2	
	Ea	Er	Ea	Er
${}^1\text{GS}_\text{S} \rightarrow {}^1\text{GS}_\text{O}$	1.29	0.27	1.28	0.20
${}^3\text{MLCT}_\text{S} \rightarrow {}^3\text{MLCT}_\text{O}$	0.45	-0.27	0.36	-0.19
${}^1\text{GS}_\text{O} \rightarrow {}^1\text{GS}_\text{S}$	1.01	-0.27	1.08	-0.20
${}^3\text{MLCT}_\text{O} \rightarrow {}^3\text{LF}_\text{O}$	0.56	0.42	0.41	0.28

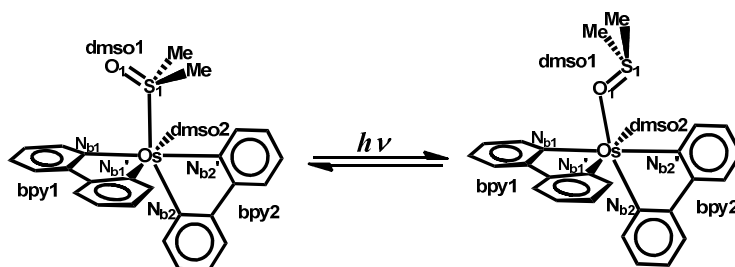


**Figure 1.** Chemical structures of the S-bonded (left) and O-bonded (right) isomers of  $[\text{Os}(\text{bpy})_2(\text{DMSO})_2]^{2+}$  complexes with the labeling scheme used throughout this work.

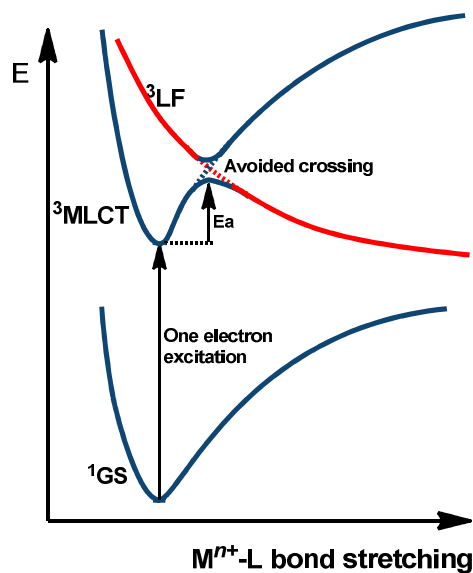


**Figure 2.** Model potential-energy curves of the ground state and two relevant excited triplet states of transition metal ( $M^{n+}$ ) complexes along the stretching of one  $M^{n+}$ -L bond between surrounding ligand and  $M^{n+}$  center (see text for a detailed description).

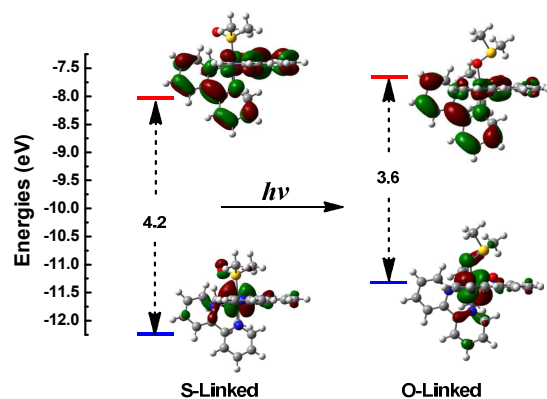


**Figure 3.** Chemical structures of the S-bonded (left) and O-bonded (right) isomers of  $[\text{Os}(\text{bpy})_2(\text{DMSO})_2]^{2+}$  complexes with the labeling scheme used throughout this work.

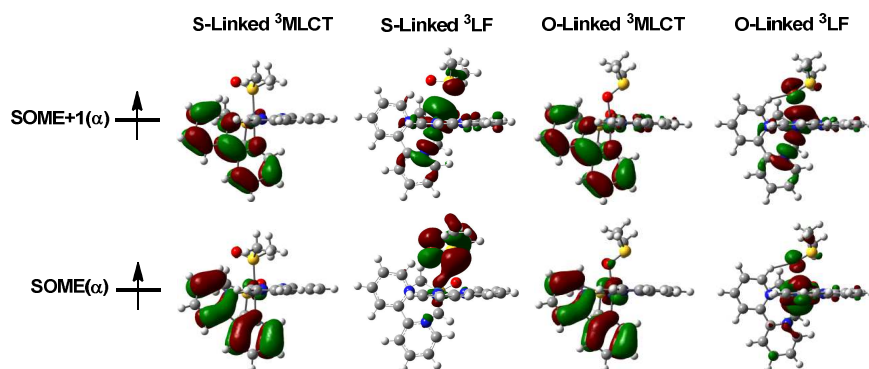


**Figure 4.** Electron configuration for the singly occupied molecular orbitals of the excited states of  $[\text{Os}(\text{bpy})_2(\text{DMSO})_2]^{2+}$ .

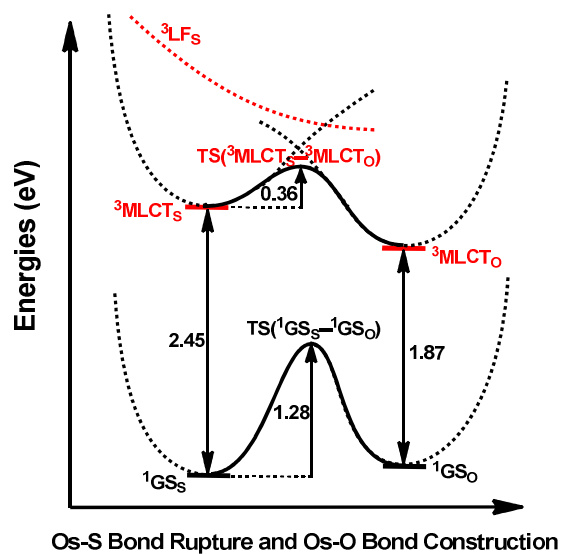


**Figure 5.** Calculated Reaction pathways for the Os-S<sub>1</sub> to Os-O<sub>1</sub> isomerization of  $[\text{Os}(\text{bpy})_2(\text{DMSO})_2]^{2+}$ . Energies are in eV.

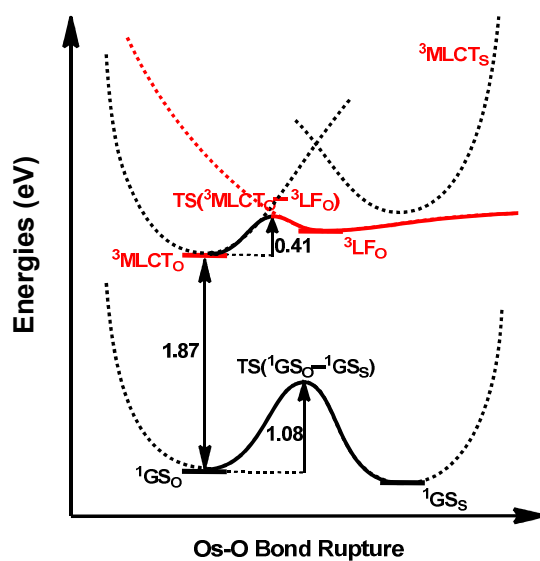


**Figure 6.** Calculated Reaction pathways for the Os-O<sub>1</sub> bond breaking process in  $[\text{Os}(\text{bpy})_2(\text{DMSO})_2]^{2+}$ . Energies are in eV.

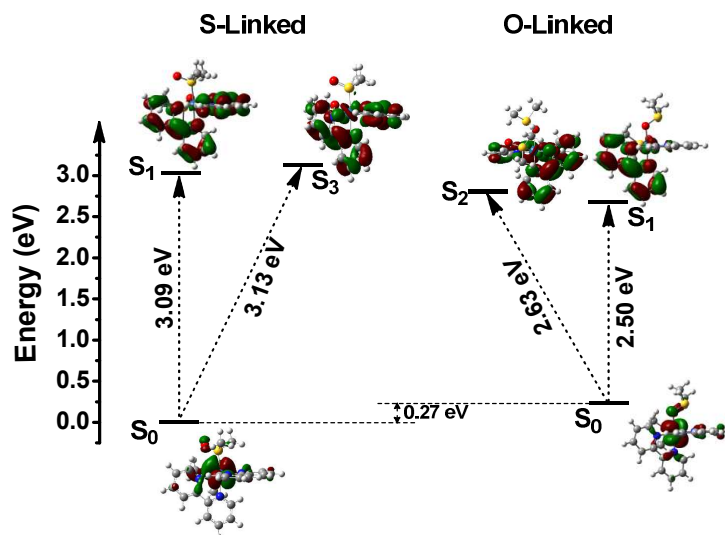


**Figure 7.** Photophysical properties of  $[\text{Os}(\text{bpy})_2(\text{dmsO})_2]^{2+}$  isomers obtained from TD-DFT calculations. The nature of the orbitals involved in the relevant excited states is also included.